Properties of laser-induced gratings in Eu-doped glasses

Edward G. Behrens, Frederic M. Durville,* and Richard C. Powell
Department of Physics, Oklahoma State University, Stillwater, Oklahoma 74078-0444

Douglas H. Blackburn
National Institute of Standards and Technology, Gaithersburg, Maryland 20894
(Received 25 August 1988; revised manuscript received 20 October 1988)

The properties of permanent, laser-induced gratings were studied in Eu^{3+}-doped glasses. These gratings are associated with a structural modification of the glass host in the local environment of the Eu^{3+} ions, and we have investigated the effects produced by altering the Eu^{3+} concentration and by changing the composition of the glass host. A two-level-system model is developed to explain the results.

I. INTRODUCTION

We have previously reported the observation of permanent, laser-induced refractive-index gratings in Eu^{3+}-doped glasses using four-wave-mixing (FWM) techniques.[1-3] These gratings were established using crossed write beams in resonance with the $^7F_0$-$^5D_2$ absorption transition of the Eu^{3+} ion and displayed buildup times of the order of 15 min. The grating is stable at room temperature but can be erased thermally by heating the sample to temperatures above room temperature or it can be erased optically with a single beam tuned in resonance with the $^7F_0$-$^5D_2$ transition of the Eu^{3+} ion. No grating formation or erasure occurs if the laser beams are not in resonance with the $^7F_0$-$^5D_2$ absorption transition of the Eu^{3+} ion.

A model was proposed to explain these gratings in which the network former and network modifier ions of the glass host can arrange themselves into two different configurations in the local environment of the Eu^{3+} ion. This leads to double-minimum potential wells for the Eu^{3+} electronic energy levels. It is assumed that the material possesses a different index of refraction depending on which configuration is present. When the Eu^{3+} ion relaxes nonradiatively from the $^5D_2$ level to the $^5D_0$ level several high-energy "phonons" are created. The local heating produced by the vibrational modes can produce a change in the structure of the local environment of the Eu^{3+} ion by causing the ions to move from one equilibrium configuration to the other.

In this paper we extend our previous work by looking at different hosts, altering the Eu^{3+} concentration, and varying the network modifier ion in a series of silicate glasses. Finally, the details of the two-level-system model are developed to provide a quantitative explanation of the data.

II. EXPERIMENTAL RESULTS OF SCATTERING EFFICIENCY MEASUREMENTS

A. Effects of Eu^{3+} concentration

To study the effect of the Eu^{3+}-ion concentration on the permanent, laser-induced grating, samples were obtained whose compositions varied only in the Eu^{3+} concentration. The first samples investigated were two Eu^{3+}-doped metaphosphate samples, one with a composition of 90 mol % $La(PO_3)_3$ and 10 mol % $Eu(PO_3)_3$, and the other with 50 mol % $La(PO_3)_3$ and 50 mol % $Eu(PO_3)_3$. These are labeled MP10 and MP50, respectively.

Permanent, laser-induced gratings were written in each sample at room temperature and the scattering efficiency of these gratings was measured using a HeNe laser for the read beam. The experimental configuration and procedures used were the same as those reported previously.[1] It was found that the laser-induced grating signal intensity of the MP50 sample was eight times stronger than that of the MP10 sample. This is consistent with the double-minimum potential-well model discussed below.

One other set of samples was investigated along this line, a lithium borate glass, LB15, with a composition of 75 mol % B_2O_3, 10 mol % Li_2O, and 15 mol % Eu_2O_3. It was possible to establish a permanent, laser-induced grating in this sample whereas in a previously investigated lithium borate sample, LB1, with only 1 mol % Eu_2O_3 no grating was created.

B. Effects of modifier ions

To study the effect of the network modifier ions of the host glass on the ability to produce gratings with high scattering efficiencies, five silicate glasses were obtained which had identical compositions except for one modifier ion. This modifier ion was changed through the series of alkali-metal ions Li, Na, K, Rb, and Cs. The exact compositions of these glasses are listed in Table I.

Permanent, laser-induced gratings were written in each of the five samples at room temperature and measurements were made of the scattering efficiencies using a HeNe laser for the read beam. The effective scattering efficiency, which is defined below, was found to decrease as the modifier ion was changed as Li→Na→K →Rb→Cs and the results are shown in Fig. 1 where the experimental values of the effective scattering efficiency are plotted versus the mass of the alkali-metal modifier ion. The solid line represents the best fit to the data using the theoretical treatment discussed in Sec. III.

TABLE I. Composition of silicate glass samples investigated. (Notation discussed in text.)

Sample	Sample composition (mol %) Network former	Network modifier	Eu content
LS5	70 SiO_2	15 Li_2O	5 Eu_2O_3
		5 BaO	
		5 ZnO	
NS5	70 SiO_2	15 Na_2O	5 Eu_2O_3
		5 BaO	
		5 ZnO	
KS5	70 SiO_2	15 K_2O	5 Eu_2O_3
		5 BaO	
		5 ZnO	
RS5	70 SiO_2	15 Rb_2O	5 Eu_2O_3
		5 BaO	
		5 ZnO	
CS5	70 SiO_2	15 Cs_2O	5 Eu_2O_3
		5 BaO	
		5 ZnO	

C. Fluoride glasses

Along with the other samples investigated a new fluoride glass was acquired, CLAP5, with a composition of 36.1 mol % PbF_2, 26.1 mol % CdF_2, 27.1 mol % AlF_3, 4.7 mol % LiF, and 5.0 mol % EuF_3. No permanent grating was observed in this sample. This is the same result as obtained previously with other fluoride glasses.[1,3]

The lack of permanent grating formation in fluoride-glass hosts is consistent with the fact that Eu^{3+}-doped fluoride glasses have been shown[3] to exhibit a significant amount of radiative emission from the ^5D_J levels above $^5D_0$. This results in fewer ions relaxing nonradiatively from the $^5D_2$ and $^5D_1$ levels to the $^5D_0$ metastable state leading to a smaller number of high-energy "phonons" being available. Since it is these high-energy local mode vibrations which are responsible for the formation of a permanent, laser-induced grating, no grating will be produced in these glasses.

In contrast, it was found that in a fluorophosphate glass, (FP, Schott FK-54), with 5 mol % EuF_3, it was possible to produce a permanent, laser-induced grating. This implies that the fluorophosphate glass contains enough of the characteristics of the phosphate glasses to allow formation of the permanent grating.

D. Temperature dependence of scattering efficiency

The temperature dependence of the laser-induced grating signal intensity in an EP sample was measured at temperatures above room temperature and the results were reported previously.[1] This section reports the results of measurements of the laser-induced grating signal intensity at temperatures below room temperature. To obtain the data the sample was mounted in a cryogenic refrigerator and the temperature was lowered to the desired level. Then a permanent grating was written and the scattering efficiency measured. This procedure was repeated at each temperature of interest. The laser-induced grating signal intensity is plotted versus temperature in Fig. 2.

As can be seen from the results, the trend toward higher laser-induced grating signal intensities continues at lower temperatures. However, there is a change in the slope between high and low temperatures. The solid lines in Fig. 2 describe an exponential temperature variation of the form

$$I = I_0 \exp\left[\frac{\Delta}{k_B T}\right], \tag{1}$$

where Δ is the activation energy. The values obtained for

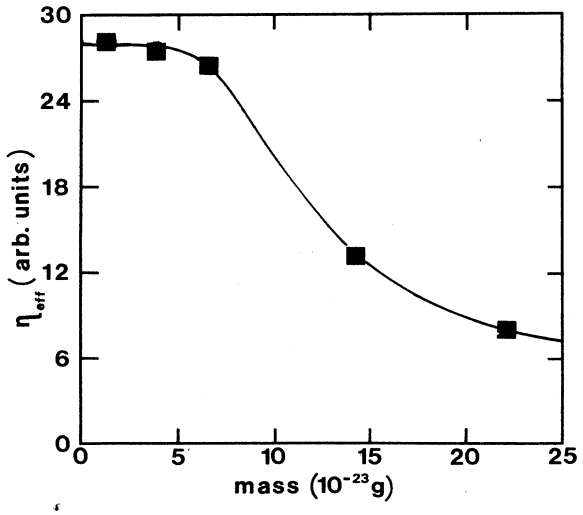

FIG. 1. Scattering efficiency of the samples listed in Table I as a function of the mass of the alkali-metal ion. ■, experimental points; ——, theoretical points.

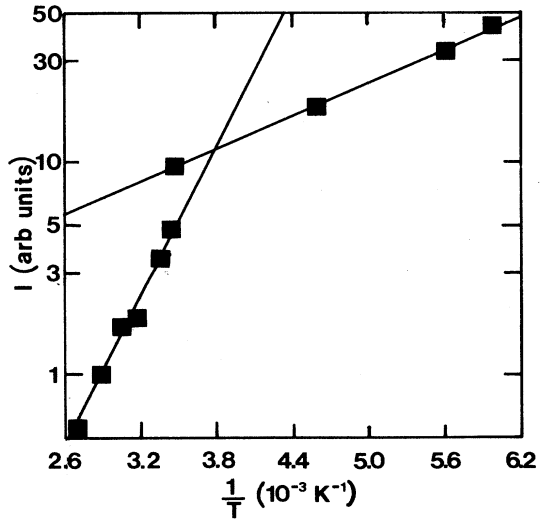

FIG. 2. Intensity of signal beam of the EP sample as a function of temperature.

Δ in the high-temperature and low-temperature regions are 2219 and 189.6 cm^{-1}, respectively.

III. THEORETICAL MODEL

In the double-minimum potential-well model the network former and network modifier ions of the glass host can arrange themselves in two possible configurations in the local environment of the Eu^{3+} ion. Thus these ions or groups of these ions have available to them two mutually accessible equilibrium positions and move in a potential of the form shown in Fig. 3. In this model it is assumed that the index of refraction depends on which configuration is present. Thus the total index of refraction of the material will be of the form

$$n = n_{\mathrm{I}} N_{\mathrm{I}} + n_{\mathrm{II}} N_{\mathrm{II}} , \tag{2}$$

where $N_{\mathrm{I\,(II)}}$ is the population of well I (II) and $n_{\mathrm{I\,(II)}}$ is the index of refraction per ion populating the well. When the laser beam is turned on the population of the wells will display a time dependence of the form

$$\frac{dN_{\mathrm{I}}(t)}{dt} = -p_{\mathrm{I}} N_{\mathrm{I}}(t) + p_{\mathrm{II}} N_{\mathrm{II}}(t) , \tag{3}$$

$$\frac{dN_{\mathrm{II}}(t)}{dt} = p_{\mathrm{I}} N_{\mathrm{I}}(t) - p_{\mathrm{II}} N_{\mathrm{II}}(t) , \tag{4}$$

where $p_{\mathrm{I\,(II)}}$ is the jump frequency and is the probability per unit time that the ion will have enough energy to jump from well I (II) to well II (I). In these experiments the system is allowed to reach equilibrium before measurements are taken. Thus the population of each well can be taken as constant and Eqs. (3) and (4) give the ratio of the populations of the two wells as

$$\frac{N_{\mathrm{I}}(\infty)}{N_{\mathrm{II}}(\infty)} = \frac{p_{\mathrm{II}}}{p_{\mathrm{I}}} , \tag{5}$$

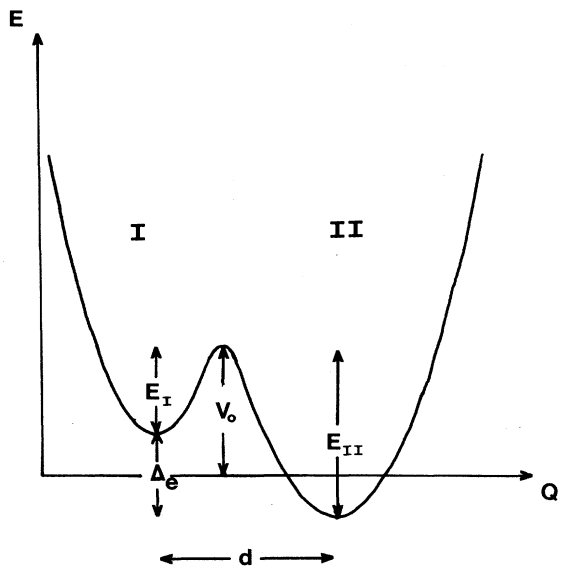

FIG. 3. Model two-level system.

where $p_{\mathrm{I,II}}$ is given by[4]

$$p_{\mathrm{I,II}} = \nu_{\mathrm{I,II}} \exp\left[-\frac{E_{\mathrm{I,II}}}{k_B T} \right] . \tag{6}$$

k_B is Boltzmann's constant and $\nu_{\mathrm{I,II}}$ is the attack frequency which is the number of attempts the ion makes at surmounting the barrier of height $E_{\mathrm{I,II}}$. Equations (5) and (6) lead to the thermal equilibrium condition

$$\frac{N_{\mathrm{I}}(\infty)}{N_{\mathrm{II}}(\infty)} = \frac{\nu_{\mathrm{II}}}{\nu_{\mathrm{I}}} \exp\left[-\frac{\Delta_e}{k_B T} \right] , \tag{7}$$

where $\Delta_e = E_{\mathrm{II}} - E_{\mathrm{I}}$. The equations derived so far are completely general and are valid for single-beam or crossed-beam experiments.

For crossed beams the intensity of the laser-induced grating signal is given by[5]

$$\mathrm{I} \propto |n_p - n_v|^2 , \tag{8}$$

where n_p and n_v refer to the index of refraction of the peak and valley regions of the laser-induced grating with

$$n_p = n_{\mathrm{I}} N_{\mathrm{I}p}(\infty) + n_{\mathrm{II}} N_{\mathrm{II}p}(\infty) , \tag{9}$$

$$n_v = n_{\mathrm{I}} N_{\mathrm{I}v}(\infty) . \tag{10}$$

The p and v subscripts refer to the peak and valley regions of the laser-induced grating whereas the I and II subscripts refer to the potential well occupied. In arriving at Eq. (10) it is assumed that the ions in the valley region of the grating remain in well I for all times. These equations lead to the following expression for the laser-induced grating signal intensity:

$$\mathrm{I} \propto |N_{\mathrm{II}p}(\infty) \Delta n_{\mathrm{II-I}}|^2 , \tag{11}$$

where $\Delta n_{\mathrm{II-I}} \equiv n_{\mathrm{II}} - n_{\mathrm{I}}$. By using the thermal equilibrium condition and the fact that the total population of the wells must remain constant, the laser-induced grating signal intensity can be written as

$$\mathrm{I} \propto \frac{N_{\mathrm{I}}^2(0) |\Delta n_{\mathrm{II-I}}|^2}{\left[1 + \frac{\nu_{\mathrm{II}}}{\nu_{\mathrm{I}}} \exp\left[\frac{-\Delta_e}{k_B T} \right] \right]^2} , \tag{12}$$

where $N_{\mathrm{I}}(0)$ is defined as $N_{\mathrm{I}p}(0) = N_{\mathrm{I}v}(0) \equiv N_{\mathrm{I}}(0)$.

This model can be used to interpret the observed changes in laser-induced grating signal intensities. For the MP50 sample and the MP10 sample the only difference will be in the initial population of configuration I. The ratio of the laser-induced grating signal intensities will be given by

$$\frac{I_{50}}{I_{10}} \propto \left[\frac{N_{\mathrm{I}}(0)_{50}}{N_{\mathrm{I}}(0)_{10}} \right]^2 . \tag{13}$$

This ratio of the squares of the initial populations was calculated using the Eu^{3+} concentration and the size of the peak region of the grating and was found to be 56.33. This number is larger than the measured ratio of eight, however, taking into consideration the simplicity of the model which does not include any saturation effects

which have been seen in power dependence measurements,[1] the model does a fairly good job in predicting the relative change in laser-induced grating signal intensities with a change in Eu^{3+} concentration.

This model can also be used to explain the results shown in Fig. 1. Since the only component of these glasses which has changed is the alkali-metal ion and it is seen that the effective scattering efficiency varies as the mass of this alkali-metal ion, this alkali-metal ion can be taken as the ion that is moving to provide the double-equilibrium configuration surrounding the Eu^{3+} ion. In Eq. (12), $N_{\rm I}(0)$, which is the initial population of well I, will depend on the size of the peak or valley regions of the laser-induced grating. Therefore, the effective scattering efficiency is defined as

$$\eta_{\rm eff}\equiv\frac{I}{N_{\rm I}^2(0)}\propto\frac{|\Delta n_{\rm II-I}|^2}{\left[1+\frac{\nu_{\rm II}}{\nu_{\rm I}}\exp\left[\frac{-\Delta_e}{k_BT}\right]\right]^2}\ . \tag{14}$$

The attack frequency $\nu_{\rm I,II}$ is proportional to the mass of the ion in the well and can be expressed as

$$\nu_{\rm I,II}=\left[\frac{k_{\rm I,II}}{m}\right]^{1/2}\ , \tag{15}$$

where $k_{\rm I,II}$ is the force constant of well I,II, respectively, and m is the mass of the ion populating the well. $\Delta n_{\rm II-I}$ is the change in refractive index per ion and is treated as an adjustable parameter. The term Δ_e which is the difference in the minima of the potential wells can be expressed more specifically using the mathematical formalism developed to describe a double-minimum potential well.[6]

Basis states $|\phi_1\rangle$ and $|\phi_2\rangle$ are chosen which are ground states for the appropriate single-well potentials. These basis states are eigenstates of the Hamiltonian of the unperturbed system H_0 with eigenvalues E_1 and E_2,

$$H_0|\phi_1\rangle=E_1|\phi_1\rangle\ , \tag{16}$$

$$H_0|\phi_2\rangle=E_2|\phi_2\rangle\ . \tag{17}$$

Upon applying a perturbation W which couples $|\phi_1\rangle$ and $|\phi_2\rangle$ the Hamiltonian matrix will become

$$(H)=\begin{bmatrix}E_1+\langle\phi_1|W|\phi_1\rangle & \langle\phi_1|H|\phi_2\rangle\\ \langle\phi_2|H|\phi_1\rangle & E_2+\langle\phi_2|W|\phi_2\rangle\end{bmatrix}\ . \tag{18}$$

To a good approximation $\langle\phi_i|W|\phi_i\rangle\ll E_i$. Defining the zero of energy to be midway between E_1 and E_2 the Hamiltonian matrix will become

$$(H)=\frac{1}{2}\begin{bmatrix}\Delta_e & \Delta_0\\ \Delta_0 & -\Delta_e\end{bmatrix}\ , \tag{19}$$

where Δ_0 is defined as

$$\Delta_0=2\langle\phi_1|H|\phi_2\rangle\ . \tag{20}$$

$\Delta_0/2$ is the coupling energy and is the difference between the two lowest symmetric states. The solution for the coupling energy is derived in a number of quantum mechanics text books and is given by[7]

$$\Delta_0=\hbar\omega_0\exp\left[-d\left[\frac{2mV_0}{\hbar^2}\right]^{1/2}\right]\ , \tag{21}$$

where $\hbar\omega_0$ is an energy roughly equal to the zero-point energy and will vary as $1/\sqrt{m}$. For this reason we can write

$$\Delta_0=\hbar\left[\frac{k}{m}\right]^{1/2}\exp\left[-d\left[\frac{2mV_0}{\hbar^2}\right]^{1/2}\right]\ , \tag{22}$$

where k is the force constant for the initial configuration.

The coupling energy can be related to the asymmetry by[8]

$$\tan\theta=\frac{\Delta_0}{\Delta_e}\ , \tag{23}$$

where θ is a measure of the mixing of the original eigenstates due to the perturbation. Combining Eqs. (22) and (23) gives

$$\Delta_e=\frac{\hbar}{\tan\theta}\left[\frac{k}{m}\right]^{1/2}\exp\left[-d\left[\frac{2mV_0}{\hbar^2}\right]^{1/2}\right]\ . \tag{24}$$

Inserting this into Eq. (14), the effective scattering efficiency becomes

$$\eta_{\rm eff}\propto\frac{|\Delta n_{\rm II-I}|^2}{\left[1+\frac{\nu_{\rm II}}{\nu_{\rm I}}\exp\left\{\frac{-\hbar}{k_BT\tan\theta}\left[\frac{k}{m}\right]^{1/2}\exp\left[-d\left[\frac{2mV_0}{\hbar^2}\right]^{1/2}\right]\right\}\right]^2}\ . \tag{25}$$

Equation (25) was fitted to the experimental values of the effective scattering efficiency with $|\Delta n_{\rm II-I}|^2$, $\nu_{\rm II}/\nu_{\rm I}$, $\hbar\sqrt{k}/k_BT\tan\theta$, and $d(2V_0/\hbar^2)^{1/2}$ treated as adjustable parameters. The best fit to the data is the solid line plotted in Fig. 1 where the following values were found for the adjustable parameters:

$$|\Delta n_{\mathrm{II-I}}|^2 = 2.787\times10^{-37} ,$$

$$\frac{\nu_{\mathrm{II}}}{\nu_{\mathrm{I}}} = 1.329 ,$$

$$\frac{\hbar\sqrt{k}}{k_B T\tan\theta} = 2.25\times10^{10} g^{1/2} ,$$

$$d\left[\frac{2V_0}{\hbar^2}\right]^{1/2} = 2.39\times10^{11} g^{-1/2} .$$

It is seen that as an ion moves from one potential well to the other the index of refraction changes by 5.279×10^{-19}. The number of ions that accumulate in well II is of the order of 1×10^{15}. This gives a total change in the index of refraction of 5.279×10^{-3}. This number is of a similar order of magnitude to that found in other experiments.[9]

From the ratio of the attack frequencies the relationship between the force constants of the individual well can be found. From Eq. (15) it is seen that

$$\frac{\nu_{\mathrm{II}}}{\nu_{\mathrm{I}}} = \left[\frac{k_{\mathrm{II}}}{k_{\mathrm{I}}}\right]^{1/2} . \tag{26}$$

It is seen that the force constant for well II, k_{II}, is 1.329 times larger than that for well I, k_{I}.

It is also possible to approximate the distance between the two wells, d, using the last parameter. From Fig. 3 it is seen that V_0 must be as large as $\Delta_e/2$. Taking V_0 to range from 3000 cm^{-1} for LS5 to 45 cm^{-1} for CS5 leads to values of d from 0.023 to 0.189 Å, respectively. It should be remembered that this model has considered only the alkali-metal ion to be the source of the double-minimum potential well. There are realistically many ions involved and the small values for d suggest that even though individual ions may move over large distances, the net effect on the configuration coordinate is minimal in moving between equilibrium configurations.

From the final two adjustable parameters it is possible to calculate Δ_e for each sample using Eq. (24). These values are listed in Table II. It is observed that as the mass of the network modifier ion increases there is a dramatic change in the asymmetry. As this ion becomes heavier the difference in the minima of the two wells becomes less, implying that the change in the local environment of the Eu^{3+} ion becomes less pronounced as you go as Li→Na→K→Rb→Cs. It has been reported that in binary alkali silicate glasses the glass becomes more ordered as the radius of the alkali-metal ion increases.[10] This same trend would be expected to continue in these glasses and as the glass becomes more ordered there would be less opportunity for multiple configurations leading to a smaller asymmetry between the two potential wells.

From Eq. (7) and the fact that the initial population of well I must equal the final population of well I and well II, it is possible to find the final populations of the two wells for each sample. These populations along with the ratio of the final population of well II to the initial population of well I are given in Table II. This ratio can be interpreted as the relative effectiveness of moving an ion initially in well I to well II. It is observed that in LS5, NS5, and KS5 almost 100% of the ions are driven into well II. In RS5 and CS5 a majority will end up in well II, however, it is a much smaller number than in the first three. In the heavier alkali-metal glasses it is harder to trap the ions in well II, implying the change in local environment of the Eu^{3+} ions is less than in the lighter alkali-metal glasses.

The inability to produce a laser-induced grating in fluoride glasses is also consistent with the double-minimum potential-well model which requires the presence of high-energy "phonons" to enable the ions to surmount the barrier and hop from well I to well II. With the absence of the high-energy local mode vibrations produced by radiationless relaxation of the Eu^{3+} ions the ions remain trapped in well I and no grating will be produced.

Finally, the temperature variation of the laser-induced grating signal intensity can be explained using the same model. Solving Eq. (7) for $N_{\mathrm{II}p}(\infty)$ and substituting directly into Eq. (11) leads to the following equation for the laser-induced grating signal intensity:

$$I \propto N_{\mathrm{I}}^2(\infty)\Delta n_{\mathrm{II-I}}^2\left[\frac{\nu_{\mathrm{I}}}{\nu_{\mathrm{II}}}\right]^2 \exp\left[\frac{2\Delta_e}{k_B T}\right] . \tag{27}$$

Thus the measured activation energy is half the asymmetry. From Sec. II D the activation energy was measured to be 2219 cm^{-1} leading to an asymmetry of 1109.5 cm^{-1} for the high-temperature case. Even though this glass is different than the silicate glasses discussed above it is seen that the asymmetry is of the same order. The low-temperature activation energy was found to be 189.6 cm^{-1}, giving an asymmetry of 94.8 cm^{-1}. This suggests that as the temperature is lowered the minima of the two wells approach each other implying that the difference in energy of the ions in each well at low temperature is not

TABLE II. Summary of parameters.

Sample	Δ_e (cm^{-1})	$N_{\mathrm{I}}(0)$	$N_{\mathrm{I}}(\infty)$	$N_{\mathrm{II}}(\infty)$	$\frac{N_{\mathrm{II}}(\infty)}{N_{\mathrm{I}}(0)}$
LS5	6068.38	1.041×10^{16}	0	1.041×10^{16}	1.00
NS5	1714.43	1.809×10^{16}	1.0×10^{13}	1.808×10^{16}	0.999
KS5	838.61	0.815×10^{16}	1.81×10^{14}	7.969×10^{15}	0.978
RS5	225.84	0.718×10^{16}	2.21×10^{15}	4.972×10^{15}	0.692
CS5	89.69	0.442×10^{16}	2.04×10^{15}	2.376×10^{15}	0.538

as great as at high temperature. This leads to the conclusion that at low temperature the local structure around each Eu^{3+} ion is close to the same in each configuration. This seems to be reasonable since at low temperature you would expect the structure to resist changes to a new configuration whereas at high temperatures the changes are more likely.

IV. DISCUSSION AND CONCLUSIONS

The double-minimum potential-well model used to describe the formation of the permanent, laser-induced grating agrees well with experimental results. It also provides some insight into the physical processes involved in the formation and erasure of these gratings. However, caution must be used in the interpretation of the physical parameters since a simple model is being used to describe a complex and poorly understood physical system.

The Eu^{3+} ions play a major role by providing the high-energy local mode phonons required to produce a structural modification of the glass host. The strength of the grating which can be produced is proportional to the concentration of Eu^{3+} ions, however, at high Eu^{3+} concentrations saturation effects occur.

The structure of the glass host in the local environment of the Eu^{3+} ions is also important to the formation of the grating. By changing one of the network modifier ions, variations in the laser-induced grating signal intensity can be produced.

As a simple model consider the glass to consist of point masses connected by springs. These point masses have available to them two equilibrium configurations which result from a change in position or a change in the force constants of the springs to which they are attached. Independent measurements have shown the elastic constants of the glasses to decrease from LS5 to CS5.[11] This implies that the two equilibrium configurations will be more stable in the lighter alkali-metal glasses than in the heavier ones. This will result in a larger value of $N_{II}(\infty)/N_I(0)$ in the lighter alkali-metal glasses than in the heavier alkali-metal glasses and is what is observed in Table II.

Stronger elastic constants also suggest there will be less displacement of the ions in the lighter alkali-metal glasses. This is exactly what was calculated in Sec. III where it was found that d ranged from 0.023 Å for LS5 to 0.189 Å for CS5. Also in Sec. III it was discovered that the ratio of k_{II} to k_I was 1.329. Since k_I decreases from LS5 to CS5, $\Delta k = k_{II} - k_I$ will also decrease from the lighter to the heavier alkali-metal-ion glasses. This suggests that Δ_e should be largest in LS5 and decrease to its smallest value in CS5. However, the actual physical displacement of the ions increases from LS5 to CS5 and suggests Δ_e should increase from LS5 to CS5. In order to form a permanent, laser-induced grating whose signal intensity decreases for LS5 to CS5 as seen in Fig. 1, Δ_e must decrease from LS5 to CS5. Therefore, the change in force constants must dominate over the change in position.

Measurements of the temperature dependence of the laser-induced grating signal intensity provides a direct means of obtaining the asymmetry and verifying the two-level-system model. For the glasses investigated in this paper the asymmetries, as found by the two methods, were of the same order of magnitude. Lowering the sample temperature results in a decrease in the asymmetry suggesting that as the temperature decreases the glasses begin to resist changes to their structure.

All of the above results are important when considering these glasses for potential optical devices. Even though much more is understood concerning the formation of the grating, the exact structure of the glass host is still unclear. Knowledge of this structure will lead to a better understanding of the processes involved.

ACKNOWLEDGMENTS

This research was supported by the U.S. Army Research Office.

---

*Permanent address: S.A. Laser Application Industrielle et Commerciale, Recherches et Systems, Z.I. Sainte Elisabeth, Montceau 71300, France.

[1]F. M. Durville, E. G. Behrens, and R. C. Powell, Phys. Rev. B **34**, 4213 (1986); E. G. Behrens, F. M. Durville, and R. C. Powell, Opt. Lett. **11**, 653 (1986).

[2]R. C. Powell, F. M. Durville, E. G. Behrens, and G. S. Dixon, J. Lumin. **40-41**, 68 (1988).

[3]F. M. Durville, E. G. Behrens, and R. C. Powell, Phys. Rev. B **35**, 4109 (1987).

[4]C. Kittel, in *Introduction to Solid State Physics* (Wiley, New York, 1976).

[5]H. Kogelnik, Bell Syst. Tech. J. **48**, 2909 (1969).

[6]W. A. Phillips, in *Amorphous Solids. Low Temperature Properties,* Vol. 24 of *Topics in Current Physics,* edited by W. A. Phillips (Springer-Verlag, Berlin, 1981), p. 1.

[7]D. Park, in *Introduction to the Quantum Theory* (McGraw-Hill, New York, 1964), p. 100.

[8]W. A. Phillips, J. Low-Temp. Phys. **4**, 351 (1972).

[9]F. M. Durville and R. C. Powell, J. Opt. Soc. Am. Ser. B **7**, 1934 (1987).

[10]S. A. Brawer and W. B. White, J. Chem. Phys. **63**, 2421 (1975); S. Brawer, Phys. Rev. B **11**, 3173 (1975).

[11]J. P. Wicksted and G. W. Gangwere (private communication).